Journal of Research in Forestry, Wildlife & Environment Vol. 12(3) September, 2020
E-mail: jrfwe2019@gmail.com; jfewr@yahoo.com
http://www.ajol.info/index.php/jrfwe
jfewr ©2020 - jfewr Publications
ISBN: 2141 – 1778
Mshelia et al., 2020

SPECTRAL RADIOMETRIC TECHNIQUE FOR CARBON ESTIMATION IN OMO FOREST RESERVE, SOUTH WESTERN, NIGERIA

***Mshelia Z. H.[1], Bamgboye, A. I. [2] and Onilude, M. A.[3]**

[1]Institute of Life and Earth Sciences (including Health and Agriculture), Pan African University, University of Ibadan, Nigeria
[2]Department of Agricultural and Environmental Engineering, University of Ibadan, Nigeria
[3]Department of Wood Product Engineering, University of Ibadan, Nigeria
***Corresponding Author:** zackmshelia@gmail.com; +234 803 644 2027

ABSTRACT

Field-estimated above-ground biomass (AGB) and spectral data from remote sensing were collected from randomly selected 50 sample plots. AGB was estimated through the biomass density equation. Radiometric measurements were carried out using a set of spectral vegetation indices. The remote sensing data was calibrated with those obtained from the field using GPS points. The average model-based estimation using satellite image canopy cover was 30.71 t/plot, while the multispectral data was 69.07 t/plot in the biosphere. This gave a difference of 1.44 t/plot and 36.91 t/plot respectively from the calculated carbon 32.16 t/plot. The canopy cover based estimation deviated from the ground measurement with 1.44 t/plot, while the estimation based on vegetation indices was twice that of field measurement. The result indicated that calibrated field measurements with forest canopy cover from high resolution image was the most reliable remote sensing technique in estimating AGB in a natural forest as compared to vegetation index. The model selected for a single tree forest based on modified soil adjusted vegetation index with value of 61.18 t/plot compared to the calculated value of 49.84 t/plot may to some extent improve AGB estimation.

Keywords: Carbon sink, Biosphere, Above-ground biomass, Vegetation index and Remote sensing

INTRODUCTION

Managing carbon deposits of forests is a valid step to mitigating world climate change (Manrique *et al*, 2012). Deforestation and forest degradation contributes significantly to increased global concentration of CO_2 in the atmosphere causing a change in global climate (IPCC, 2007). The forest emits carbon through burning, degradation, deforestation, decomposition and sinks atmospheric carbon by means of photosynthesis and plant development (Boschetti *et al.*, 2007). Carbon represents 50% of the biomass (IPCC, 2000) and the knowledge of the processes involved in the storage and the release of carbon in terms of scale and time from earthly habitats still needs to be improved (Keith *et al.*, 2009; Manrique *et al*, 2012).

In Nigeria, 9.7 million hectares (about 10%) of the total land mass of the country, consists of forest reserves and only a small portion of this forest is lowland rainforest. In the late 1990s it was estimated that only 1.19 million hectares of lowland rainforest remained in the country and about 288,000 hectares of which was designated as official forest reserves (ITTO, 2011; Salami *et al*., 2016).

Spectral records from sensors have shown good relationships with the biomass in different regions (Lu *et al*., 2004; Anaya *et al*., 2009). Also, good relations have been reported between field-estimated spectral records and different biophysical attributes of forest (Grant *et al*., 2007). Geospatial techniques are recently being used in the study of forest ecosystems (Fernández *et al*., 2010). However, few studies were found to have estimated AGB with the combination of radiometric signals from remote sensing data and AGB field survey.

The spectral reflectance data is usually transformed into spectral vegetation indices (VI), in form of mathematical models used to measure the spectral contribution of vegetation in multispectral observations (Nikolaos *et al.*, 2006; Manrique, *et al.*, 2012). Several VIs were correlated with biophysical vegetation parameters and with biomass (Foody *et al*., 2003; Soenen *et al.*, 2010). Some of the best known VIs often used for monitoring biomass, are, the Normalized Difference Vegetation Index (NDVI), Transformed Soil-Adjusted Vegetation Index (TSAVI), Modified Soil-Adjusted Vegetation Index ($MSAVI_2$), Ratio Vegetation Index (RVI), and Advanced vegetation (AVI) (Foody *et al*., 2003; Soenen *et al*., 2010; Thenkabail *et al*., 2002).

The focus of this paper is to estimate carbon, specifically in terms of above-ground biomass with the specific objectives to conduct a field measurement to determine tree parameters and compare Carbon from the field measurements and estimation from remote sensing data. The study develops a reliable methodology which integrates the data mentioned above in a Geographic Information System (GIS), which allows modelling and mapping of the AGB and carbon present in a mosaic natural and single tree forests

MATERIALS AND METHODS

Study Area

The Omo Forest Biosphere Reserve, which derives its name from River Omo that traverses it, is located north of Sunmoge, between latitudes 6^o 42' to 7^o 05' N and longitude 4^o 12' to 4^o 35' E (Fig 1) in the Ijebu area of Ogun State in South-western Nigeria. Omo covers about 130,500 hectares, which includes a 460 ha Strict Nature Reserve (Okali and Ola-Adams 1987). The climate is tropical in nature and it is characterized by wet and dry seasons. The temperature ranges between 21 and 34°C while the annual rainfall ranges between 150 and 3000 mm (Larinde *et al*., 2011; Adedeji *et al*., 2015).

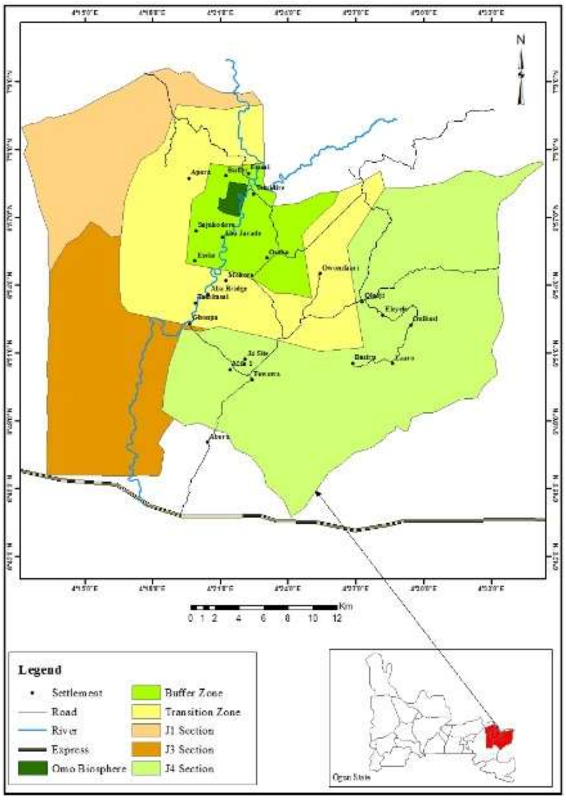

Figure1: Map of Omo Forest Reserve

Data Collection and Analysis

The structural variables such as diameter at breast height (DBH) $\geq$ 20 cm, tree height and wood density were recorded in the field. This structural information obtained was used to estimate the AGB, which is the total amount of living organic material of trees. Field measurement of tree variables were carried out using relaskop, haga altimeter, increment borer, scale weight, measuring tape, ranging pole and Global Positioning System (GPS). These field allometric data were acquired in January, 2018.

Landsat 8 OLI satellite image of 2018 was identified as path 190 and row 55, and used with Transverse Mercator Projection System and Datum WGS84. This image provides moderate-scale data of 30m. A high resolution image of 1m was used to extract forest canopy coverage in Omo Biosphere.

Aboveground biomass (AGB) of Omo forest reserve

To estimate the AGB, Tree Basal Area (TBA) which is the cross-sectional area (over the bark) at breast height (1.3 metres above the ground) was first calculated (equation 1). This was determined by measuring the diameter at breast height in centimeters and calculate the basal area (m^2) using an equation based on the formula for the area of a circle (area = p r^2 where r = radius and p = 3.142) where r is DBH divided by 2.

$BA(m^2) = pi * DBH(cm)^2 /4$ ...... [1]

The Volume for each tree was estimated using the Newton's formula

$$V = \pi H\left(\frac{Db^2 + 4Dm^2 + Dt^2}{24}\right) \text{......... [2]}$$

Where
V = Stem volume (m3),
H = total height (m),
Db = Diameter at base (cm),
Dm = Diameter at the middle (cm),
Dt = Diameter at the top (cm).
The AGTB is being calculated using equation 3
AGTB (t/ha) = Volume of tree (m^3/ha) × Wood specific density (t/m^3) x Biomass Expansion Factor (5)
(3)

Where:
BEF= Exp {(3.213 – 0.506*Ln (BV)} for BV < 190 t/ha …… [4]
When BV > = 190 t/ha, a constant of 1.74
Where
BV= Biomass Volume (t/ha) = Volume per hectare (m^3/ha) x Average wood density (t/m^3) .. [5

Where Biomass Volume **(BV)** = Vol/ha x Average Density....... [6]
and average density calculated thus

$$\text{Average Density} = \frac{Total\ Tree\ Density\,(g/cm^3)}{Total\ number\ of\ trees} \text{ …. [7]}$$

Carbon (C) stock was derived from aboveground biomass by assuming that nearly 50% of the biomass is made up by carbon (IPCC, 2006 and Hung et al, 2012).
C = Biomass (t/ha) ∗ 0.5 ….. [8]

The weight of carbon dioxide in trees is determined by the ratio of CO_2 to C which is 44/12 (Kauffman & Donato, 2012). Carbon dioxide was calculated as follows:

CO_2 = Carbon (t C/ha) ∗ 44/12 ….. [9]

Sub-pixel based Carbon Estimation

To achieve this, satellite image obtained was subjected to basic adjustments or pre-processing. This pre-processing is necessary to adjust the data for use in quantitative analysis (Agbor *et al*, 2018) such as radiometric correction. Radiometric error of the Landsat satellite image of 2018 were verified to ensure data quality using ArcGIS 10.5. The images used in this study were first converted to Top of Atmosphere (TOA) radiance using equation 10 (Giannini *et al.*, 2015).

$$L\lambda = \left(\frac{(L_{MAX}\lambda - L_{MIN}\lambda)}{Q_{CAL}\lambda}\right) Q_{CAL} + L_{MIN}\lambda \text{ …… [10]}$$

Where:
$L\lambda$ =Spectral radiance at the sensor's aperture [W/(m^2 sr µm)]
Q_{CAL} = Quantized calibrated pixel value [DN]
Q_{CAL}MIN = Minimum quantized calibrated pixel value corresponding to $L_{MIN}\lambda$ [DN]
Q_{CAL}MAX = Maximum quantized calibrated pixel value corresponding to $L_{MAX}\boldsymbol{\lambda}$) [DN]
$L_{MIN}\ \lambda$ = Spectral at-sensor radiance that is scaled to Q_{CAL}MIN [W/(m^2 sr µm)]
LMAX, = Spectral at-sensor radiance that is scaled to Qcalmax [W/ (m 2 sr µm)].
The above expression does not consider the atmospheric effects, therefore there is need to convert images from radiance to reflectance measures, using equation 11 ((Giannini *et al.*, 2015).

$$\rho^{\lambda} = \frac{\pi * TOAr * d^2}{E_{Esun^{\lambda}} * \text{Cos}\,\theta_{sz}} \quad \ldots\ldots [11]$$

Where:
$\rho\lambda$ = Planetary TOA reflectance (unitless)
π= mathematical constant approximately equal to 3.14159 (unitless)
$L\lambda$ = spectral radiance at the sensors aperture [w/(m^2 sr µm)]
d^2 = the earth-Sun distance (Astronomical unit)
E_{SUN} = mean exoatmospheric solar irradiance [w/(m^2 sr µm)].
θ_{SZ}= the solar zenith angle (degree). The cosine of this angle is equal to the sine of the sun elevation θ_{SE}. That is, $\theta_{SZ} = \cos(90 - \theta_{SE})$.

These are rescaling factors given in metadata.
The grid referencing system of individual bands of each of the images used have been transformed to one reference system (WGS1984 UTM Zone 31N). The re-projection is important to make accurate analysis of the datasets and comparability possible. For the satellite analysis of the sample plots, we extracted the reflectance in the respective bands of the image of Landsat 8 OLI. This study utilized Maximum Likelihood classification Algorithm and spectral values based on Vegetation indices and band ratios, as integral part of the classification processes. The results of these operations make classification of the study area in pixels into different land cover types relatively easy.

Image classification generally involves labeling the pixels as belonging to particular spectral class using the spectral data available. It is assumed in this study that the spectral classes for an image be represented by ω_i and the pixel as x. To determine the class or category to which a pixel x belongs; it is strictly the conditional probabilities $p(\omega i \mid x)$. This is the probability that the class (ωi) is the correct for a pixel at position x where

$i = 1 \ldots m$ …. [12]
m = total number of classes.
The image classification will be performed according to
$x \in \omega i$, if ….. [13]
$p(\omega i \mid x) > p(\omega j \mid x)$ for all $j \neq I$ ……… [14]

This means that the pixel at position x belongs to class ω_i if $p(\omega_i \mid x)$ is the largest. One major problem that associates with this classifier is that $p(\omega i \mid x)$ are not always known. To estimate a probability distribution for a land cover type (i.e. a class) that describes the chance of finding a pixel from class ωi at position x ($i.e.\, p(x \mid \omega i)$, this study ensured that sufficient training samples are available as recommended by (John *et al*, 2006). They recommend as a practical minimum that $10N$ training pixels per spectral class be used, where N is the number of channels. The dimensionality of data (images) that will be used in this research is low (3-channel multispectral images), therefore achieving these numbers will not be impossible.

Forest Canopy Analysis

30 plots of 30m x 30m boundary was overlay on a high resolution of 1m and the forest cover was digitalized. The area of the digitized forest cover was calculated to determine the area cover of the tree crown. Figure 3 shows selected plots used for canopy cover analysis in Omo Biosphere.

Forest cover assessment by Vegetation Indices

The Normalized Difference Vegetation Index is defined as

$$NDVI = \frac{Nir_{\lambda} - \text{Re}\,d_{\lambda}}{\text{Nir}_{\lambda} + \text{Red}_{\lambda}} \quad \ldots\ldots.. [15]$$

This was introduced by Rouse *et al*. in1974 in order to produce a spectral VI that separates green vegetation from its background soil brightness using Landsat digital data (Nikolaos *et al.*, 2006). It is expressed as the difference between the near infrared and red bands normalized by the sum of those bands. It is the most commonly used VI as it retains the ability to minimize topographic effects while producing a linear measurement scale. In addition, division by zero errors is significantly reduced. NDVI values will typically range between -1 and 1 where the higher the value, the healthier and denser the vegetation (Makinde *et al.*, 2018).

The Advance Vegetation Index (AVI), which is highly sensitive to forest density and physiognomic vegetation classes, was also used im estimating carbon stock from satellite image. AVI was calculated using equation 4 (Agbor *et al*, 2018).

$$AVI = \sqrt[3]{\{(B6+1)(65536-B4)(B5-B4)\}} \quad \ldots\ldots [16]$$

Where B = Band

Another widely used VI is the Ratio Vegetation Index (RVI), which was adopted in this study and calculated as shown in the following equation 15.

$$RVI = \frac{Nir_\lambda}{Red_\lambda} \quad \ldots\ldots [17]$$

Another index used is the $TSAVI_2$ (Transformed Soil-Adjusted Vegetation Index) is a VI that considers a correction factor to compensate for the relative effect of the soil, and to take into account the observed amount of vegetation. It was propounded by Baret and Guyot, in 1991 (Nikolaos et al, 2006) and is calculated using equation 18.

$$TSAVI2 = \frac{a(Nir - aR - b)}{R + aNIR - ab + 0.08\,(1 + a^2)} \quad \ldots\ldots [18]$$

Where NIR = reflectance in the near infrared band (expressed as reflectances), R = reflectance in the visible red band (expressed as reflectances), a = slope of the soil line and b = intercept of the soil line. The final index used is the $MSAVI_2$. This is the second modified SAVI introduced by Qi, et al., 1994 which uses an inductive *L* factor to remove the soil "noise" that was not canceled out by the product of NDVI and correct values greater than 1 that SAVI may have due to the low negative value of NDVI (Nikolaos et al, 2006). The general expression of $MSAVI_2$ is given as equation 19.

$$MSAVI_2 = \frac{2_{\rho_{nir}} + 1 - \sqrt{(2_{\rho_{nir}} + 1)^2 - 8(\rho_{nir} - \rho_{Red})}}{2} \quad \ldots\ldots [19]$$

ρ_{nir} = reflectance of the near infrared band (expressed as reflectances)

ρ_{Red} = reflectance of the red band (expressed as reflectances)

Regression Analysis

AGB and spectral (VI) data were used to derive and evaluate a set of predictive relations for AGB estimation from remote sensing. For all data, the correlations between AGB and VI, as well as those between the different VI (field and satellite), were assessed using regression equation expressed as in equation 20.

$$y = a + mx \quad \ldots\ldots [20]$$

Where:

y = the measured variable

a = the intercept

m = the rate of change and

x = the VI.

The data with more statistically significant relationships and higher correlation coefficient was selected to model the AGB in the forest reserve. The simulated biomass was compared with field data. For validation of the estimated AGB, we used 30 randomly selected field plots to model biomass distribution and 20 plots whose biomass was compare with the predicted biomass.

RESULTS

Aboveground biomass (AGB) of Omo forest reserve

A total of eight hundred and one (801) trees of twenty three (23) families and sixty five species of DBH ≥ 20cm were enumerated in the study area as shown in table 1.

Table 1: Data distribution according to family and number of tree species

S/No.	Family	No. of Species	No of Observation	%
1	Annonaceae	4	25	3.12
2	Apocynaceae	3	44	5.49
3	Bignoniaceae	1	1	0.12
4	Boraginaceae	1	30	3.75
5	Cannabaceae	2	18	2.25
6	Combretaceae	2	8	1
7	Ebenaceae	5	70	8.74
8	Euphorbiaceae	7	116	14.5
9	Fabaceae	5	17	2.12
10	Malvaceae	8	126	15.7
11	Meliaceae	5	40	4.99
12	Moraceae	1	8	1
13	Myristicaceae	1	19	2.37
14	Olacaceae	1	130	16.2
15	Phyllanthaceae	2	2	0.25
16	Putranjavaceae	7	81	10.1
17	Rubiaceae	3	24	3
18	Ruscaceae	1	2	0.25
19	Rutaceae	1	3	0.37
20	Sapindaceae	1	1	0.12
21	Sterculiacae	1	1	0.12
22	Tiliaceae	2	30	3.75
23	Urticaceae	1	5	0.62
	Total	65	801	100

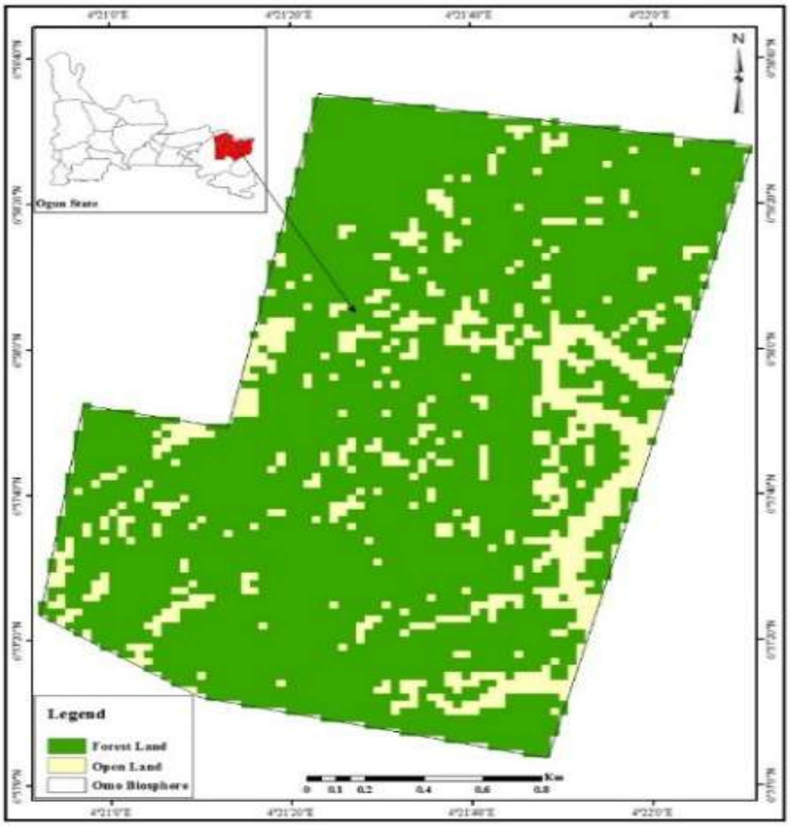

Figure 2: Forest cover of Omo Biosphere

Table 1: Forest cover Statistics of Omo Biosphere Reserve.

Category	Area m	Area ha	%
Forest cover	4169	375.21	89
Open land	499	44.91	11
Total	4668	420.12	100

Figure 2, shows the forest cover of Omo biosphere with the colour green showing the area covered by forest and colour yellow are areas of non-forest which were the mosaic of water body and open land. The image was classified into forest and open land for ease of estimation of the actual carbon stock in the study area. Table 1 indicates that the area covered by forest in the biosphere is 89%, while non-forest is 11%, covering 375.21 ha and 44.91 ha respectively.

Table 2 Summary of Forest Carbon Stock Estimation from Sampled Plots

Parameter	AGB (t/ha)	Carbon stock (t/ha)	C02 (t/ha)
Mean	737.93	368.97	1354.10
Minimum	21.28	10.64	39.04
Maximum	1765.67	882.84	3240.01
Sum	36896.58	18448.29	67705.22

Table 2 shows the summary of the above ground biomass (AGB), carbon stock and carbon dioxide calculated from the 50 sampled plots in Omo biosphere reserve. The estimated net biomass of the stems ranges from 21.28 to 1765.67 ton/ha with a mean of 737.93ton/ha; the carbon stock ranges from 10.64 to 882.84 ton/ha with a mean of 368.97 ton/ha; and the CO_2 sequestered ranges from 39.04 to 3240.01 ton/ha with a mean of 1354.10 ton/ha (Table 2).

Since the actual area of Omo biosphere reserve under forest is 375.21 ha, the carbon content of the reserve is estimated as: 375.21 (ha) x 368.97 (t/ha). Estimated Carbon Content of the Reserve = 138,441.24 tons. Estimated CO_2 Content of the Reserve = 138,441.24 x 3.67 = 508,079.33 tons

Therefore, estimated net carbon stock of the stems of the Omo biosphere is 138,441.24 tons while the CO_2 equivalent is 508,079.33 tons. The study determined that Omo biosphere reserve has great capacity to sink carbon and it can also emit CO_2 about four times into the environment than the amount it sinks when it undergoes deforestation and degradation. This shows the important of sustainable forest management as a measure to mitigate the impact of climate change.

Table 2: Linear Relationships between Estimated Biomass and Vegetation Indices

Vegetation Indices	Equation	R^2: plantation	R^2: natural forest
NDVI		0.29	0.001
$MSAVI_2$		0.32	0.033
AVI		0.29	0.001
TSAVI1	Linear	0.30	0.001
RVI		-0.29	0.007
Forest Canopy		-	0.75

The relationships between the vegetation indices obtained from satellite data shown in table 2 indicated a weak relationship between VIs and the biomass. The Omo biosphere with dense vegetation of different trees species had the poorest values of all indices with $MSAVI_2$ having the highest value. Boschetti *et al*. (2007) established that NDVI exhibits low fidelity with the above-ground biomass in heterogeneous forest. In contrast, the relationship improved in the site that is characterised by single tree species (*Gmelina arborea*) with AVI, NDVI, $MSAVI2_2$, TSAVI and RVI. The best fitting index proved to be the $MSAVI_2$, as asserted by other authors in the monitoring of vegetation (Julien *et al*., 2009).

Table 3: Derived Models to Assess and Map AGB in Omo Biosphere and Plantation

Model	Equations	R	Forest type	Independent variable	Dependent variable
1	$y = -106.13 + 0.1731x$	0.75	Natural forest	Forest canopy	Estimated biomass
2	$y = -15.316 + 191.43x$	0.03		$MSAVI2_2$	Estimated biomass
3	y = 145.78x - 21.203	0.32	Plantation forest	$MSAVI2_2$	Estimated biomass

Vegetation Indices and forest canopy based estimated AGB

Vegetation indices were introduced to estimate carbon by sub-pixels. The regression model obtained described the relationship between calculated AGB from the field data and VI ($MSAVI2_2$). The regression produced a coefficient of the independent variable ($MSAVI_2$) and an intercept value indicating the state of the dependent variable (calculated AGB) when the independent variable is zero. To estimate the AGB by pixels, the $MSAVI_2$ images served as the independent variable(x) in equations 2 and 3 (table 3). Adding the product of the images and the coefficient to the constant (a) produce the value of y for each pixel. The established equations between the values of forest canopy and AGB was linear (r^2=0.75). The distribution of biomass showed a lower range as compared to estimation based on vegetation indices in the natural forest of Omo biosphere (Table 3).

Forest Canopy Analysis

30 plots of 30m x 30m boundary was overlay on a high resolution of 1m and the forest cover was digitalized. The area of the digitized forest cover was calculated to determine the area cover of the tree crown. Figure 2 shows selected plots used for canopy cover analysis in Omo Biosphere.

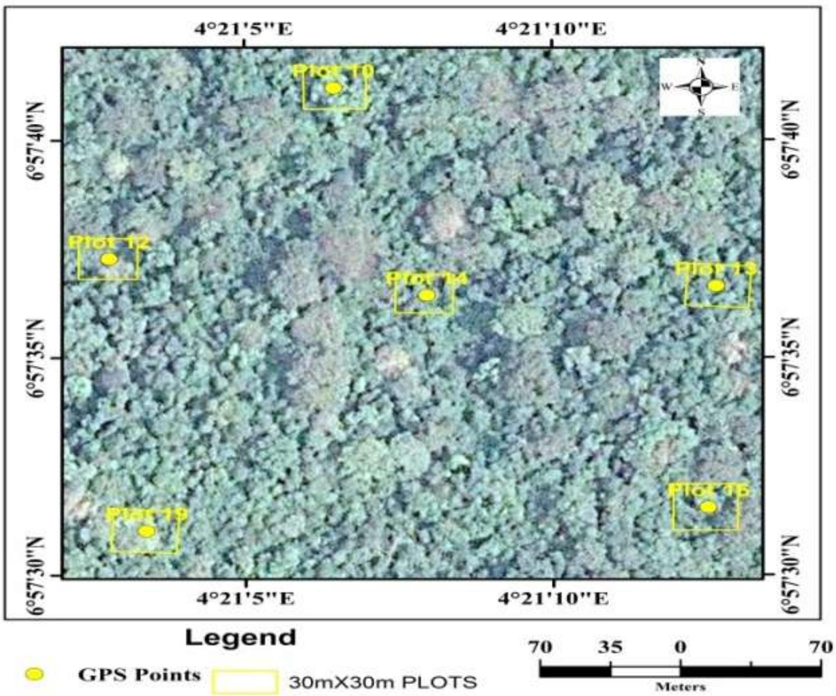

Figure 3: Selected plots within Omo forest reserve on high resolution image

Adopting tree canopy as a way to determine biomass became necessary because of mixed pixels present in Landsat images used. This increases the level of uncertainty in biomass estimation from the coarse images that can be minimized using a finer resolution image such as Google archived image (figure 3). It provides a more reliable carbon estimates and relates better with ground data than lower resolution image used for radiometric estimates.

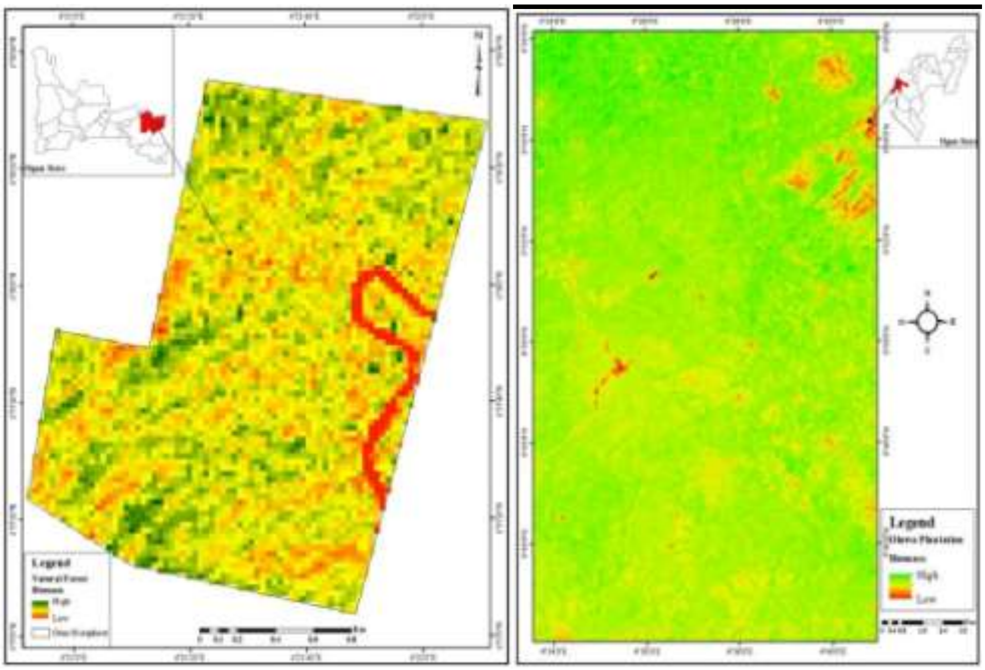

(a) (b)

Figure 4: Sub-pixel distribution of AGB (t/ha) for (a) Natural forest and, (b) Single specie plantation using models 2 and 3

The images in figure 4 are the outputs of the simulation exercises from model 2 and 3 in table 3. Figure 4a is an AGB distribution map of Omo biosphere. The dark green colour shows areas of high biomass with colour red as areas of low biomass or no biomass (compared with land cover in figure 2). The same is applicable to figure 4b as dark green has higher biomass while the red areas are areas of low or no biomass. The new pixel values of biomass extracted from Omo Biosphere and forest plantation (figure 4) after the simulation and data from forest canopy analysis were compared with the calculated data of the 20 plots set aside for validation and the results is in table 4.

Table 4: Mean Estimated Carbon of Selected Plots

Location	Density	Volume m^2	Calculated Carbon	Estimated Carbon by VI	Estimated Carbon by Canopy area
Natural forest	2.71	12.44	33.72	70.07	32.71
Plantation	4.2	11.87	49.84	61.18	-

The calculated carbon in the natural forest was 33.72 t/plot and the derived carbon based on vegetation index was 70.07 t/plot. The estimation of carbon based on canopy area gives a closer value of 32.71 t/plot. Applying the same indices in a single tree ecosystem, derived carbon was closer to calculated value especially with modified soil adjusted vegetation index as shown in table 4.

DISCUSSION

Integration of the plot measurements with remote sensed data was used to developed regression models for estimating AGB over the whole study area. However, the use of vegetation indices over estimates AGB in the study area while the high resolution image gives a closer result to the calculated. The inconsistences with the use of vegetation indices could be as result of the mixture of spectral component such as trees, soil, and shade in a pixel of an image which is captured as signature or one pixel. The limitation of pixed-based vegetation indices or reflectance values for estimating AGB was addressed using canopy based model. The high resolution image of 1m used in the canopy based model was able to differentiate clearly forest and non-forest, thereby enhancing the accuracy of the estimation.

Plantation forest was added mainly for the assessment and verification of model from the natural forest. The P-value of .004, reveal that there are no statistically significant differences between the AGB field data surveyed and the AGB data estimated using model 1. Other models, especially the VI overestimates the AGB of both forest reserves, though more unpredictable in natural forest. As important as forest carbon measurement is, applying the method that reduces error is necessary for proper monitouring and management of the forest.

CONCLUSION

This study showed that spectral records from satellite radiometry are an important source of input to estimate the aboveground biomass of each site. $MSAVI2_2$ is the index that best explains the relationships between AGB and vegetation reflectance. The most reliable remote sensing technique to estimate AGB in a natural forest is by using forest canopy cover from high resolution image rather than vegetation index. The model selected for a single tree forest based on modified soil adjusted vegetation index can to some extent improve AGB estimation detail and proper monitoring of such data.

Acknowledgement

This work is supported financially by the African Union under the Pan African University scholarship and Forestry Research Institute of Nigeria for the use of the Omo Strict Nature Reserve.

REFERENCES

Adedeji, O. H., Tope-Ajayi, O.O., and Abegunde, O.L. (2015). 'Assessing and Predicting Changes in the Status of Gambari Forest Reserve, Nigeria Using Remote Sensing and GIS Techniques'. *Journal of Geographic Information System*, 7, 301-318.

Agbor C.F, Makinde EO (2018) Land surface temperature mapping using geoinformation techniques. *Geoinf FCE CTU* 15:17. https://doi.org/10.14311/gi.17.1.2

Boschetti, M.; Bocchi, S. and Brivio, P.A. (2007): "Assessment of pasture production in the Italian Alps using spectrometric and remote sensing information". *Agriculture, Ecosystems and Environment*, 118: 267–272.

Fernández, N.; Paruelo, J.M. and Delibes, M. (2010): "Ecosystem functioning of protected and altered Mediterranean environments: A remote sensing classification in Doñana, Spain". *Remote Sensing of Environment*, 114: 211–220.

Giannini M. B., O. R. Belfiore, C. Parente and R. Santamaria (2015). Land Surface Temperature from Landsat 5 TM images: comparison of different methods using airborne thermal data measurements and comparison with MODIS remote sensing estimates." *Agricultural and Forest Meteorology* 129: 151- 173. https://doi.org/10.1007/s12665-019-8433-7.

Grant, J.P.; Wigneron, J.P.; Van de Griend, A.; Kruszewski, A.; Søbjærg, S., and Skou, N. (2007): "A field experiment on microwave forest radiometry: L-band signal behaviour for varying conditions of surface wetness". *Remote Sensing of Environment*, 109: 10–19.

Intergovernmental Panel on Climate Change-IPCC (2007): "The physical science basis". In: Climate Change 2007. Contribution of Working Group I to the Fourth Assessment. Solomon, S., Qin, M., Manning, Z., Chen, M., Marquis, K.B., Averyt, M., Miller, H. Eds. Cambridge University Press, Cambridge, United Kingdom

Intergovernmental Panel on Climate Change-IPCC, (2000) – Nebojsa Nakicenovic and Rob Swart (Eds.) Cambridge University Press, UK. Pp570.

ITTO. (2011). 'Status of Tropical Forest Management'. Technical series 38:420.

Julien, Y. and Sobrino, J.A. (2009). The yearly land cover dynamics (YLCD) method: an analysis of global vegetation from NDVI and LST parameters. Remote Sensing of Environment, 113: 329 - 334.

Kauffman, J.B., & Donato, D.C. (2012). Protocols for the measurement, monitoring and reporting of structure, biomass and carbon stocks in mangrove forests. Working Paper 86. CIFOR, Bogor, Indonesia.

Keith, H.; Mackey, B.G. and Lindenmayer, D.B. (2009): "Re-evaluation of forest biomass carbon stocks and lessons from the world's most carbon-dense forests". *PNAS*, 106 (28): 11635–11640.

Larinde, S.L., & Olasupo, O.O. (2011). 'Socio-Economic Importance of Fuelwood Production in Gambari Forest Reserve Area, Oyo State, Nigeria'. *Journal of Agriculture and Social Research (JASR)*, 11.

Manrique, S. M., Núñez, V. Franco, J. (2012): "Estimating aboveground biomass in native forest using remote sensing data combined with spectral radiometry", *GeoFocus (Artículos)*, 12: 349-373.

Nikolaos G. S, Thomas K. A , Ioannis Z. G, and Konstantinos P. (2006). Vegetation Indices: Advances Made in Biomass Estimation and Vegetation Monitoring in the Last 30 Years. *Geocarto International*, Vol. 21, No. 4, December 2006.

Okali, D. U. U. and Ola-Adams, B.A. (1987). Tree population changes in treated rain forest at Omo Forest Reserve, Nigeria. *Journal of Tropical Ecology*,3,291-313.

Salami, K. D., Akinyele, A. O., Adekola, P. J., & Odewale, M. A. (2016). 'Tree species composition and regeneration potential of Onigambari Forest Reserve, Oyo State'. vol.4 (3), pp.39-47.

Soenen, S.A.; Peddle, D.R.; Hall, R.J.; Coburn, C.A. and Hall, F.G. (2010): "Estimating aboveground forest biomass from canopy reflectance model inversion in mountainous terrain". *Remote Sensing of Environment*, 114: 1325–1337.

Thenkabail, P.S.; Enclona, E.A.; Ashton, M.S. and Van Der Meer, B. (2004): "Accuracy assessments of hyperspectral waveband performance for vegetation analysis applications". *Remote Sensing of Environment*, 91: 354-376

.